

RESEARCH ARTICLE

Circular RNAs expression profiles and bioinformatics analysis in bronchopulmonary dysplasia

Yu Lun  | Junlong Hu | Yang Zuming

Department of Neonatal Intensive Care Unit, Suzhou Municipal Hospital, Jiangsu Province, China

Correspondence

Yang Zuming, Department of Neonatal Intensive Care Unit, Suzhou Municipal Hospital, Daoqian Street NO.26, Suzhou, Jiangsu Province, 215000, China.
Email: 13915509208@163.com

Funding information

The Jiangsu Commission of Health, Grant/Award Number: F201936; The Suzhou Science and Technology Bureau, Grant/Award Number: SKJYD2021112

Abstract

Background: Bronchopulmonary dysplasia (BPD) has long been considered the most challenging chronic lung disease for neonatologists and researchers due to its complex pathological mechanisms and difficulty in prediction. Growing evidence indicates that BPD is associated with the dysregulation of circular RNAs (circRNAs). Therefore, we aimed to explore the expression profiles of circRNAs and investigate the underlying molecular network associated with BPD.

Methods: Peripheral blood was collected from very-low-birth-weight (VLBW) infants at 5–8 days of life to extract PBMCs. Microarray analysis and qRT-PCR tests were performed to determine the differentially expressed circRNAs (DEcircRNAs) between BPD and non-BPD VLBW infants. Simultaneous analysis of GSE32472 was conducted to obtain differentially expressed mRNAs (DEmRNA) from BPD infants. The miRNAs were predicted by DEcircRNAs and DEmRNAs of upregulated, respectively, and then screened for overlapping ones. GO and KEGG analysis was performed following construction of the competing endogenous RNA regulatory network (ceRNA) for further investigation.

Results: A total of 65 circRNAs (52 upregulated and 13 downregulated) were identified as DEcircRNAs between the two groups ($FC > 2.0$ and $p_{adj} < 0.05$). As a result, the ceRNA network was constructed based on three upregulated DEcircRNAs validated by qRT-PCR (*hsa_circ_0007054*, *hsa_circ_0057950*, and *hsa_circ_0120151*). Bioinformatics analysis indicated these DEcircRNAs participated in response to stimulus, IL-1 receptor activation, neutrophil activation, and metabolic pathways.

Conclusions: In VLBW infants with a high risk for developing BPD, the circRNA expression profiles in PBMCs were significantly altered in the early post-birth period, suggesting immune dysregulation caused by infection and inflammatory response already existed.

KEYWORDS

blood, bronchopulmonary dysplasia, circular RNAs, microarray analysis, VLBW infants

This is an open access article under the terms of the [Creative Commons Attribution-NonCommercial-NoDerivs](https://creativecommons.org/licenses/by-nc-nd/4.0/) License, which permits use and distribution in any medium, provided the original work is properly cited, the use is non-commercial and no modifications or adaptations are made.

© 2022 The Authors. *Journal of Clinical Laboratory Analysis* published by Wiley Periodicals LLC.

1 | INTRODUCTION

Bronchopulmonary dysplasia (BPD) is the most common chronic lung disease in neonates, especially with a high incidence rate of approximately 45% in preterm infants with a gestational age of less than 29 weeks,¹ leading to severe complications and poor long-term outcomes, including impaired pulmonary function and neurodevelopmental disorders.^{2,3} The main pathological changes of BPD include simplified alveolar structures and pulmonary capillary dysplasia. In addition to barotrauma and volutrauma, oxygen toxicity, fluid overload, and genetic factors, the immature lung may also suffer damage due to infection or inflammatory response.^{4,5} A complex etiology and perplexing pathogenesis have led to an absence of specific biomarkers for prediction and precision therapy of BPD.⁶

The rapid advancement of high-throughput microarray technologies and genome-wide sequencing techniques offers the potential for prediction, diagnosis, therapy, and pathologic insights into human diseases.⁷⁻⁹ Mounting evidence has revealed that lncRNAs and circRNAs are critical regulators of gene expression. In addition to encoding protein, circRNAs could act as sponges for miRNAs to regulate the expression of downstream mRNAs.¹⁰⁻¹² A significant advantage of circRNAs over other RNAs is their more stable structure¹³ and a longer half-life in various tissues and body fluids, making them more amenable to being specific biomarkers and therapeutic targets.^{14,15} Considering this, mounting studies have focused initially on the epigenetic perspective and, more recently, on circRNAs to explore the molecular mechanisms of BPD.¹⁶ Several studies have discovered that aberrant expression of circRNAs is associated with the pathogenesis of BPD.¹⁷⁻¹⁹ First, Zou Z et al constructed a mice model of LPS-induced lung injury to identify the different expression profiles of circRNAs. This study observed numerous significantly upregulated circRNAs accompanied by abnormally increasing TNF- α and IL-1 β in the serum. Astonishingly, after applying P2X7 receptor antagonists, the expression of circRNAs (circ_0001679 and circ_0001212) and the cytokine mRNA levels were restrained, alleviating lung damage caused by sepsis.²⁰ Another study demonstrated that circRNAs could act as miRNA sponges and subsequently regulate target gene expression correlated with lung injury. In neodymium oxide-treated human bronchial epithelial (16HBE) cells, hsa_circ_0000638 inhibited the activation of NF- κ B by competitively binding to miR-498-5p and further downregulated the expression of IL-8 and IL-1 β .¹⁸ Additionally, in the pulmonary hypertension mice models, Zhang J et al identified the ceRNA network and further verified that the circ-calm4/miR-337-3p/Myo10 signal transduction axis could modulate the proliferation of pulmonary artery smooth muscle cells.²¹ Although partially circRNAs have been implicated in the pathogenesis of BPD, further research is necessary to confirm these findings.¹⁹

Due to the difficulty of obtaining human lung tissues, peripheral blood is one of the most common substitution sources.²² A growing number of studies have recently employed gene expression profiles obtained from peripheral blood mononuclear cells (PBMCs) as both a method for pathogenesis research and a diagnostic tool for several

lung diseases.²³ As part of this study, we used microarray technology to detect the circRNA expression profiles in PBMCs between BPD and normal VLBW infants. Based on the circRNA expression profiles, DEcircRNAs were identified, and a portion with significant upregulation was further validated with qRT-PCR. Simultaneously, we obtained the DEmRNA expression profiles between BPD and non-BPD VLBW infants from GEO databases. Potential miRNAs binding to circRNAs and mRNAs were predicted for further construction of circRNA-miRNA pairs and miRNA-mRNA pairs, respectively. Finally, we constructed the circRNA-miRNA-mRNA regulatory network based on screening circRNA-miRNA pairs and miRNA-mRNA pairs with overlapped miRNAs. Gene Ontology (GO) and Kyoto Encyclopedia of Genes and Genomes (KEGG) analyses were performed to investigate the molecular function and signaling pathways affecting BPD progression. These identified DEcircRNAs and DEmRNAs obtained from moderate to severe BPD infants may provide novel insights for early disease prediction and management. The flowchart of this study is shown in [Figure 1](#).

2 | METHODS AND PATIENTS

2.1 | Ethical compliance

This study was funded by the Jiangsu Commission of Health (reference number: F201936) and the Suzhou Science and Technology Bureau (reference number: SKJYD2021112), with permission from the ethics office of the Suzhou Municipal Hospital. As guardians of each infant, both parents signed an informed consent form, and there was no harm to the infants.

2.2 | Specimen collection

PBMCs were derived from peripheral blood samples obtained from VLBW infants (birth weight <1500g and gestational age <32 weeks) born in Suzhou Municipal Hospital from May to December 2020. For each VLBW infant, 0.5 ml peripheral blood specimen was collected 5-8 days after birth. The PMBCs were separated using lymphocyte isolation solution and transferred into enzyme-free 1.5 ml EP tubes. Samples were immediately frozen at -80°C after adding the appropriate amount of TRIzol reagent (Invitrogen, United States). The entire manipulation process was completed within 2 h.

The categorized grade of BPD was defined based on the infant's requirement for oxygen and different respiratory support modalities at 36 weeks corrected gestational age (moderate BPD: oxygen requirement <30% FiO₂; severe BPD: oxygen requirement >30% FiO₂ or continuous positive airway pressure (CPAP)/mechanical ventilation).²⁴⁻²⁶

Exclusion criteria were (1) infants with chromosomal abnormalities, (2) significant congenital deformities, and (3) treated with corticosteroids in the first week of birth. Finally, three VLBW infants with moderate to severe BPD were selected as the BPD group, and three

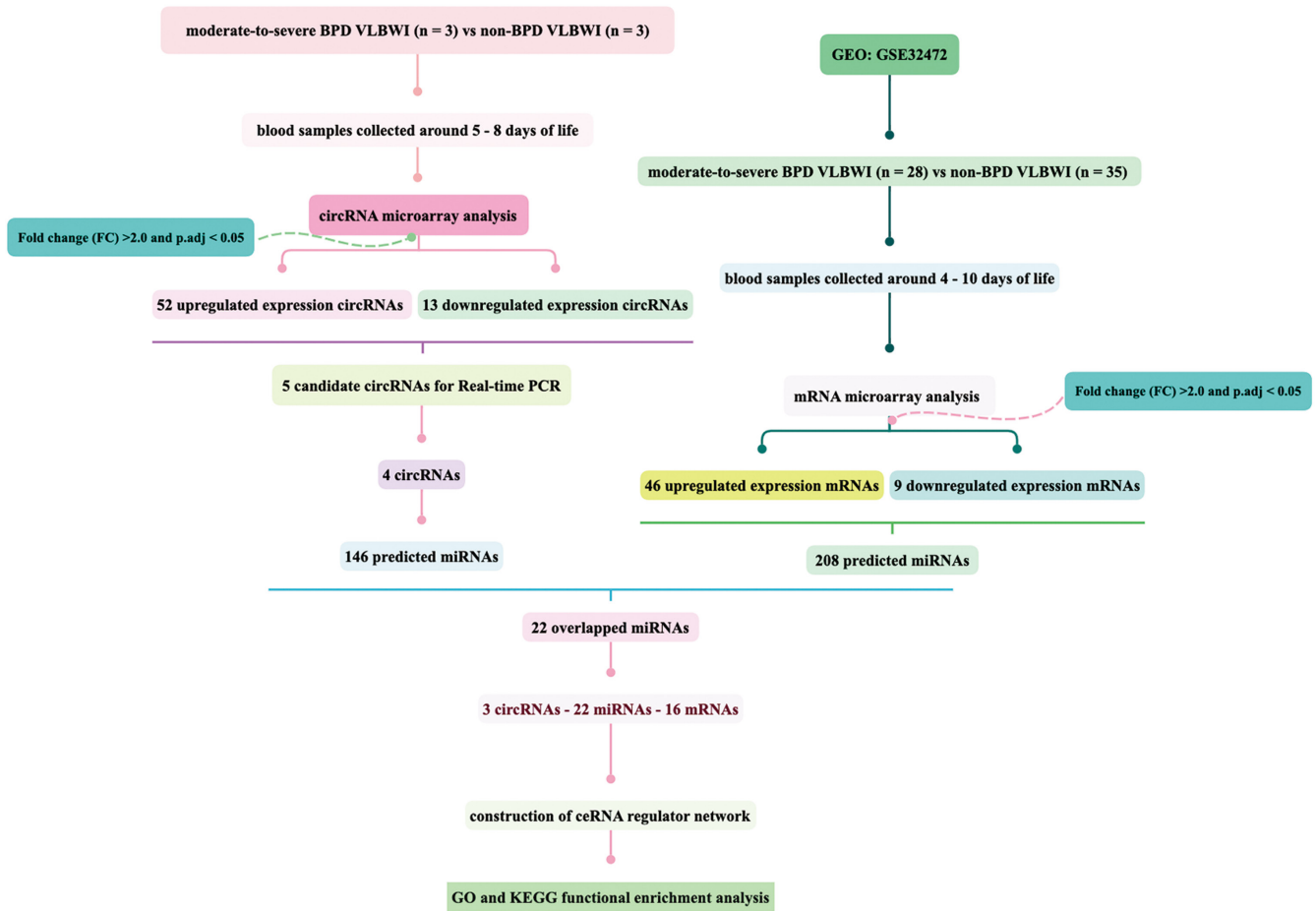


FIGURE 1 Flowcharts for study subjects.

VLBW infants with a matched gestational age of non-BPD were chosen as the control group. Basic information about these infants is shown in Table 1.

2.3 | CircRNA microarray analysis

Total RNA was extracted using the TRIzol reagent (Invitrogen, United States). The quality and quantity of the RNA samples were detected with a NanoDrop ND-1000 spectrophotometer and agarose gel electrophoresis. Only samples with OD_{260/280} ratios between 1.80 and 2.0 were selected for examination in the subsequent step. The linear RNA was digested using RNase R (Epicenter, Inc.) for isolating enriched circular RNAs.

The enriched circular RNAs were amplified and transcribed into fluorescent cRNAs using a random primer according to the Arraystar Super RNA Labeling protocol (Arraystar, Inc.). The labeled cRNAs were hybridized onto the Arraystar Human circRNA Arrays V2 (8 × 15K, Arraystar) and incubated for 17 h at 65°C in an Agilent Hybridization Oven. After washing, slides were scanned with the Agilent Scanner G2505C.

Data from microarrays were obtained through Agilent Feature Extraction software. Gene Spring V12.0 (Agilent) was used to sum

up data from the two groups. The data were quantile standardized and further processed using the R software limma package. The final normalized intensity in the analysis was derived from the log₂-transformed normalized data (Figure S1A). Employing Benjamin and Hochberg's technique, *p*-Values were adjusted to decrease false discovery rates. CircRNAs with a fold change of more than 2.0 and a *p*-Value of less than 0.05 were selected as differentially expressed genes (DECircRNAs).

2.4 | Quantitative real-time RT-PCR validation

We selected five significantly upregulated DECircRNAs (hsa_circ_0007054, hsa_circ_0057950, hsa_circ_0050386, hsa_circ_0057953, and hsa_circ_0120151) for quantitative real-time-PCR (qRT-PCR) validation. The complementary DNA (cDNA) was reverse-transcribed using SuperScript™ III Reverse Transcriptase (Invitrogen, United States). The 20 µl reaction system contained 250 ng template RNA, 1 µl Random, 1.6 µl dNTPs Mix (2.5 mM), 5 × First-Strand Buffer 4 µl, 1 µl DTT (0.1 M), 0.5 µl Rnase Inhibitor, 1 µl SuperScript III-RT (Invitrogen: 18080-044), and added to 20.0 µl with RNase-free water. QRT-PCR analyses were carried out using 2 × PCR Master Mix (Arraystar: AS-MR-006-5). NCBI Primer-BLAST

TABLE 1 Clinical characteristics of the Control and BPD group.

	Control	group	(n = 3)	BPD	group	(n = 3)	p-Value
	1#	2#	3#	1#	2#	3#	
Gestational age (w)	27+1	28	28+5	27+6	26	27+2	0.28
Birth weight (g)	1050	970	850	770	680	950	0.13
Sex gender	male	female	female	female	male	female	-
PROM	+	-	+	+	-	-	-
Preeclampsia	-	+	+	-	-	+	-
Antenatal steroids	+	+	+	+	+	+	-
Apgar 1 min	8	6	7	4	8	8	0.82
Apgar 5 min	9	9	9	8	8	9	0.11
RDS > stage 2	+	-	-	+	-	+	-
Surfactant treatment	+	+	+	+	+	+	-
Days with ventilator (d)	2	0	1	31	36	26	0.05
Days with CPAP (d)	10	21	12	42	38	39	0.05
Hospitalization days	60	73	82	92	84	74	0.13
PDA	+	-	-	-	-	-	-
IVH > stage 2	-	-	+	-	+	+	-
NEC > II B	-	-	-	-	+	-	-
EOS	-	-	-	-	-	+	-
LOS	-	-	+	-	+	+	-
VAP	-	-	-	-	+	+	-
ROP	-	+	-	-	+	-	-
Discharge weight (g)	1950	2010	2030	1980	1670	2000	0.28
Outcome	discharge	discharge	discharge	discharge	dead	discharge	-

Abbreviations: EOS, early-onset neonatal sepsis; IVH, intraventricular hemorrhage; LOS, late-onset neonatal sepsis; NEC, necrotizing enterocolitis; PDA, patent ductus arteriosus; PROM, premature rupture of membranes; RDS, respiratory distress syndrome; ROP, retinopathy of prematurity. VAP, ventilator-associated pneumonia.

and Genaray Biotech were utilized to design and manufacture all primers. The 20 μ l reaction system consisted of 2 \times Master Mix, 0.5 μ M forward and reverse primers, respectively, 100 ng template DNA, and added to 20.0 μ l with RNase-free water. The real-time-qPCR cycling protocol was initiated at 95°C for 10 min, followed by 40 cycles of 95°C for 10 s and 60°C for 1 min, and finally 95°C for 10 s, 60°C for 1 min, 95°C for 15 s. The relative expression levels of gene were calculated using the comparative Ct method ($2^{-\Delta\Delta Ct}$). All measurements were performed in triplicate, and the gene expression levels were standardized to β -actin. The primers were synthesized by Genscript Corporation, and the primer sequences are listed in Table 2.

2.5 | Microarray Data acquisition from publicly available database

We screened the GEO database for microarray sequencing analysis data that met the following criteria: (1) studies containing preterm infants of less than 32 weeks gestational age and birth weight \leq 1500 g, (2) studies with blood samples that were drawn from

infants on the 4th to 10th day of life for the assessment of gene expression in peripheral blood leukocytes, and (3) studies with a clarification of BPD severity grading (none, mild, moderate, and severe). Based on the above criteria, one data set (GSE32472)²⁷ was obtained from the GEO database. The platform used for GSE32472 is the Affymetrix Human Genome 1.0 ST Array. A total of 111 preterm infants were included in this prospective study, conducted between September 1, 2008, and November 30, 2010, in Norway and Poland.

2.6 | Identification of DEmRNAs and DE miRNAs

First, data downloaded from the GEO were preprocessed and normalized using the preprocess Core package in R version 3.6.2 (Figure S2). Then, between the moderate to severe BPD group and non-BPD group, mRNAs with a fold change $>$ 2.0 and adjusted p-value $<$ 0.05 were identified as differentially expressed (DEmRNAs).

We integrated the Circular RNA Interactome database to identify the downstream target miRNAs for each DEcircRNA and

TABLE 2 Sequences of forwarding and reverse primers

Gene	Sequence (5'-3')	Length (bp)
β -Actin	F: 5'GTGGCCGAGGACTTTGATTG3' R: 5'CCTGTAACAACGCATCTCATATT3'	73
hsa_circ_0007054	F:5'GACAAGTCCGAGGTGATAGTTACA3' R: 5'CTTTTCCCCCAGTCAATG3'	118
hsa_circ_0057953	F:5"GGTCCGTCTAATGAAGAACAGATTT3' R: 5'CGCTTTTGGGAATCAGTTACAC3'	89
hsa_circ_0050386	F: 5'TCCACCGAGATCCAGAACAGA3' R: 5'GAGTGGCGTATTCCCATTGTT3'	123
hsa_circ_0057950	F: 5'GTCCGTCTAATGAAGAACAGGTA3' R: 5'CATCTCCACTCTGCTGGTTCTC3'	71
hsa_circ_0120151	F: 5'GGAGCCAGAAGGAAGAGTGAT3' R: 5'CCCCAAGAGTCCATGATTTTA3'	140

Note: The circRNA ID is in circBase (<http://circbase.org>).

calculated the minimum free energy (MFE) via the RNAhybrid program. Simultaneously, the target miRNAs of DEmRNAs were predicted based on the miRWalk database,²⁸ the miRDB database,²⁹ and the mirDIP database.³⁰ Following that, we used Venny 2.1 (<https://bioinfogp.cnb.csic.es/tools/venny/>) to make a Venn diagram and screened for overlapping miRNAs common to these data sets.

2.7 | Construction of ceRNA network

Based on the DEcircRNAs identified after qRT-PCR validation, the overlapped prediction miRNAs, and the DEmRNAs, we constructed the circRNA-miRNA pairs and the miRNA-mRNA pairs. Subsequently, a novel circRNA-miRNA-mRNA regulatory network based on the ceRNA hypothesis was constructed using Cytoscape 3.7.1.

2.8 | GO and KEGG functional enrichment and statistical analysis

To investigate the molecular interaction and mechanism underlying the ceRNA regulatory network, we performed GO and KEGG functional enrichment analysis based on g: Profiler.³¹ For GO enrichment analysis, three components were employed for demonstrating different levels of biological functions: the molecular function (MF), the biological process (BP), and the cellular component (CC). In addition, the KEGG enrichment analysis was applied to assess the level of gene enrichment in various pathways. Based on the most significant adjusted p-value, the top five GO terms and KEGG pathways were selected.

In the primary demographic continuous data analysis, non-normally distributed data were expressed as median (M) and range (P25 - P75); normally distributed data were described as mean \pm standard deviation. In contrast, categorical data were presented as frequency (%). Wilcoxon signed rank tests or chi-square

tests were used to compare the different features between the BPD and the control groups. Data analyses were performed using Stata version 17.0 and R version 3.6.2.

3 | RESULTS

3.1 | General clinical data

Among the six VLBW infants, there was no significant difference in birth weight or gestational age between the BPD and control groups. For the BPD group, the median gestational age at birth was 27.3 (26-27.9) weeks, and the non-BPD group was 28 (27.1-28.7) weeks, and no evidence of a significant difference was found ($p = 0.28$); similarly, the median birth weight of the BPD group was 770 (680-950) g, and the non-BPD group was 970 (850-1050) g, and the distribution was still not significantly different ($p = 0.13$). Additional clinical character details of the six VLBW infants are shown in [Table 1](#).

From the GEO database of GSE32472, we screened a total of 28 VLBW infants with moderate to severe BPD and 35 VLBW infants with non-BPD based on the time of blood collection and the diagnostic grading criteria for BPD. However, the BPD group's gestational age and birth weight were significantly lower than the control group, except for gender. BPD group, the median gestational age at birth was 25.5 (24.5-27) weeks, and the non-BPD group was 29²⁸⁻³⁰ weeks; similarly, the median birth weight of the BPD group was 705 (600-910) g, and the control group was 1200 (1150-1400) g, revealing the uneven distribution of both gestational age and birth weight (p -Value = 0).

3.2 | CircRNA expression profiles

Among all the expression dysregulation circRNAs of the BPD group, 65 circRNAs were confirmed to be significantly differentially

expressed ($FC > 2.0$ and $p_{adj} < 0.05$), with 52 upregulated and 13 downregulated. We compared the samples' post-normalization expression value distributions using a box plot. Each sample's \log_2 ratio followed the same pattern. We noticed that most dysregulated circRNAs were generated by exons; the others were derived from introns and intergenic regions. In the stacked bar plot, the distribution of circRNAs on different human chromosomes was revealed (Figure 2). Volcano plots, heatmap of hierarchical clustering analysis, and scatter plots (Figure S1B) were used to illustrate the differences in circRNA expression between the two groups. The top 10 up or downregulated circRNAs are summarized in Table 3A,B.

3.3 | Quantitative Real-time RT-PCR validation

Results indicated that more upregulated circRNAs were expressed in the BPD group than downregulated ones. Thus, to confirm the findings of the circRNA microarray analysis, qRT-PCR was utilized

to validate the expression of five significantly upregulated circRNAs. Finally, four circRNAs (*hsa_circ_0007054*, *hsa_circ_0050386*, *hsa_circ_0057950*, and *hsa_circ_0120151*) were consistent with the microarray data (Figure 3); nevertheless, *hsa_circ_0057953* did not amplify by qPCR.

3.4 | Identification of DEmRNAs and DEmiRNAs

Based on the Circular RNA Interactome database and the RNAhybrid program, we predicted 146 potential target miRNAs associated with the four DEcircRNAs. Simultaneously, 55 (46 upregulated mRNAs and 9 downregulated mRNAs) DEmRNAs were identified from GSE32472 (Figure 4A,B). By taking advantage of the miWalk database, miRDB, and miRDIIP databases, we identified 208 target miRNAs associated with the 46 upregulated DEmRNAs. Eventually, we gained 22 overlapped DEmiRNAs, and 16 targeted DEmRNAs for the following research, as shown in the Venn plot and bar plot.

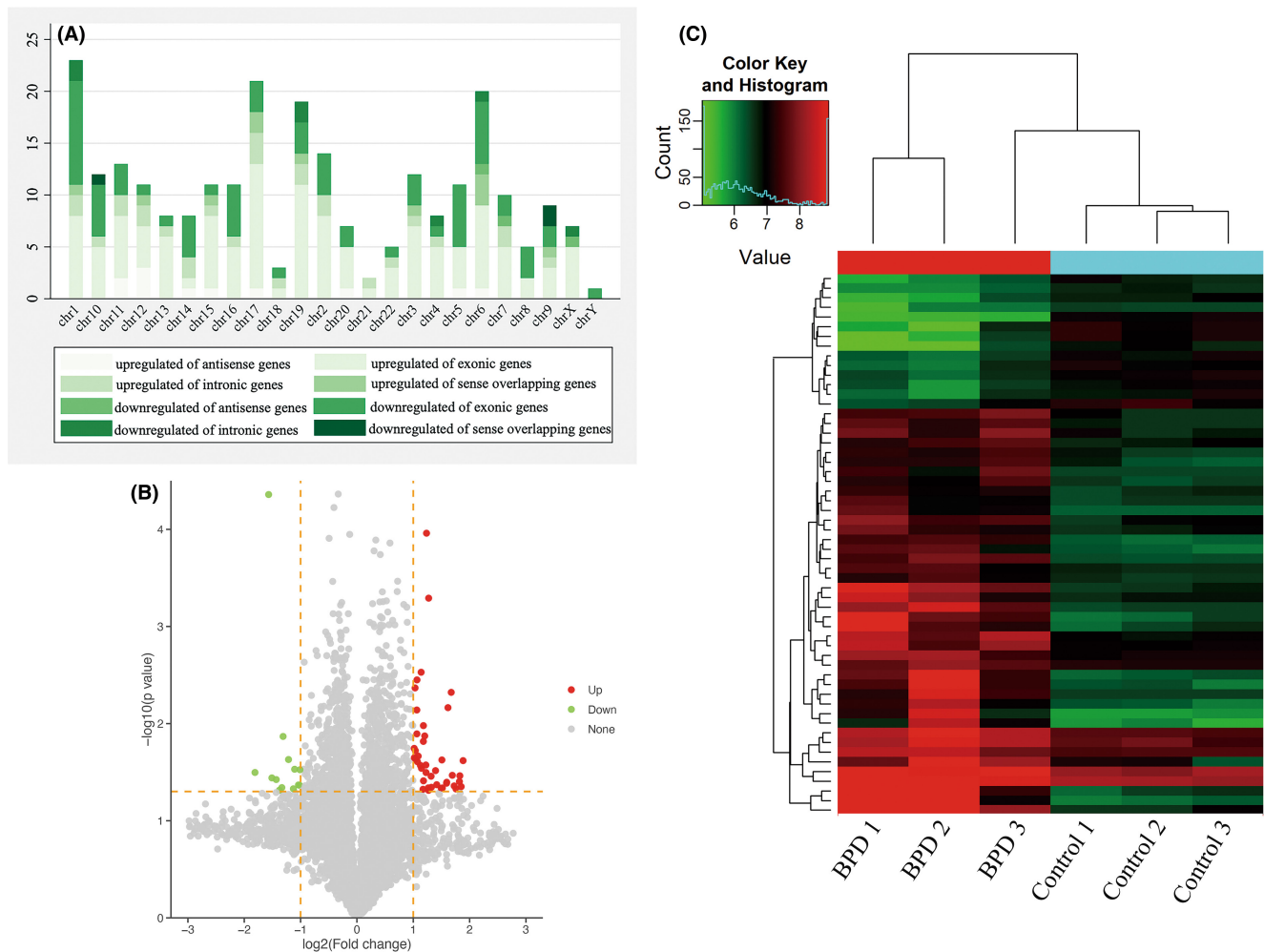


FIGURE 2 Differentially expressed circRNA between the BPD and control groups. (A) Stacked bar plot. The horizontal coordinates represent the different circRNA distribution on different chromosomes; the different colours represent the different origins of circRNA. (B) Volcano figure. The circRNAs of significance upregulated were shown with the red dots; the significance downregulated circRNAs were shown with the green dot. Fold-change > 2.0 and adjusted p -Values < 0.05 was significantly different. (C) Heatmap of hierarchical clustering analysis. CircRNAs with differential expression between the two groups were analyzed via hierarchical clustering.

TABLE 3 The top 10 (A) upregulated (B) downregulated circRNAs.

circRNA ID	chromosome	circRNA type	Gene Symbol	Fold change	P-value
(A)					
hsa_circ_0003574	chr20	exonic	GID8	2.354	<0.0001
hsa_circ_0064986	chr3	exonic	NKTR	2.093	0.0035
hsa_circ_0006752	chr22	exonic	NF2	2.045	0.0042
hsa_circ_0050386	chr19	exonic	ANKRD27	3.19	0.0048
hsa_circ_0043138	chr17	exonic	TAF15	3.065	0.0069
hsa_circ_0030448	chr13	exonic	LMO7	2.089	0.0072
hsa_circ_0057950	chr2	exonic	CREB1	2.266	0.0105
hsa_circ_0007054	chr1	exonic	TMEM50A	4.853	0.0155
hsa_circ_0045234	chr17	exonic	DDX42	2.052	0.019
hsa_circ_0043820	chr17	exonic	PTRF	2.125	0.022
(B)					
hsa_circ_0002210	chr8	exonic	ZNF706	2.847	0.03623
hsa_circ_0075819	chr6	exonic	CASC15	3.505	0.0318
hsa_circ_0001656	chr6	antisense	ARID1B	2.152	0.0295
hsa_circ_0000830	chr18	exonic	CEP192	2.518	0.0456
hsa_circ_0003608	chr1	exonic	YY1AP1	2.596	0.0485
hsa_circ_0084666	chr8	exonic	CSPP1	2.022	0.0432
hsa_circ_0020076	chr10	exonic	ABLIM1	2.32	0.0234
hsa_circ_0043815	chr17	exonic	STAT3	2.963	<0.0001
hsa_circ_0003520	chr16	exonic	NETO2	2.698	0.0377
hsa_circ_0040481	chr16	exonic	RFWD3	2.48	0.0136

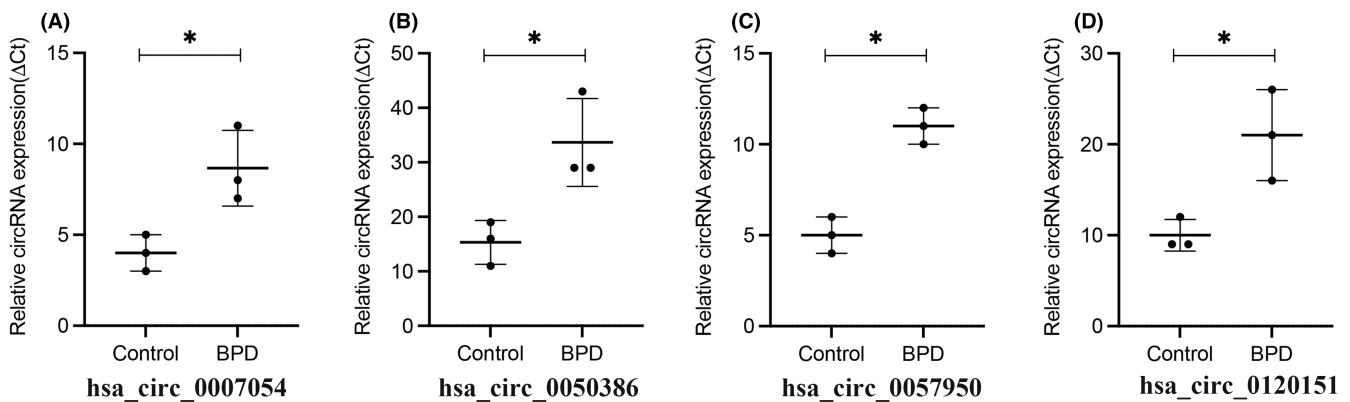


FIGURE 3 The expression levels of the circRNAs validation by qRT-PCR Gene expression was assessed using Δ Ct values, normalized to β -actin levels. Means \pm SEM was presented in the table. * $p < 0.05$.

3.5 | Construction of ceRNA network

Based on the DEcircRNAs with qRT-PCR validation and the DEmRNAs detected in GSE32472, a novel ceRNA regulatory network was established and visualized. With the identified 48 edges (22 circRNA-miRNA edges and 26 miRNA-mRNA edges) and the 41 identified nodes (3 circRNAs, 22 miRNAs, and 16 mRNAs), Cytoscape 3.7.1 software constructed the final ceRNA network as described in Figure 5.

3.6 | GO and KEGG functional enrichment analysis

GO and KEGG pathway analyses were used to annotate the function of DEmRNAs in the ceRNA network. A total of 408 GO terms and 9 KEGG pathways were significantly enriched ($p_{adj} < 0.05$), and the top 20 most significantly enriched terms and pathways are listed in Figure 6. GO biological process (BP) was mainly enriched in "immune system process," "response to external stimulus," "myeloid leukocyte activation," "response to biotic stimulus," and "neutrophil activation."

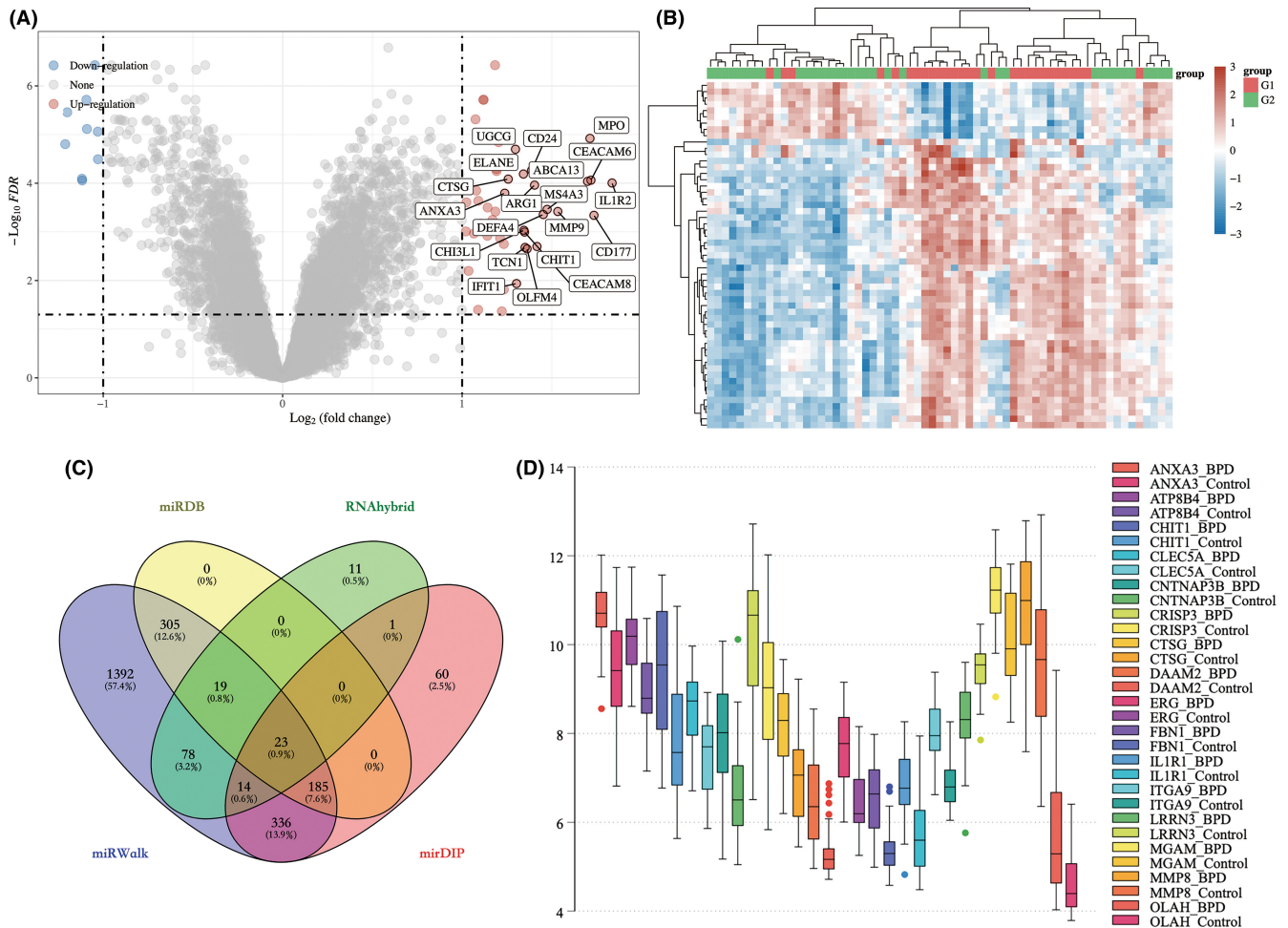


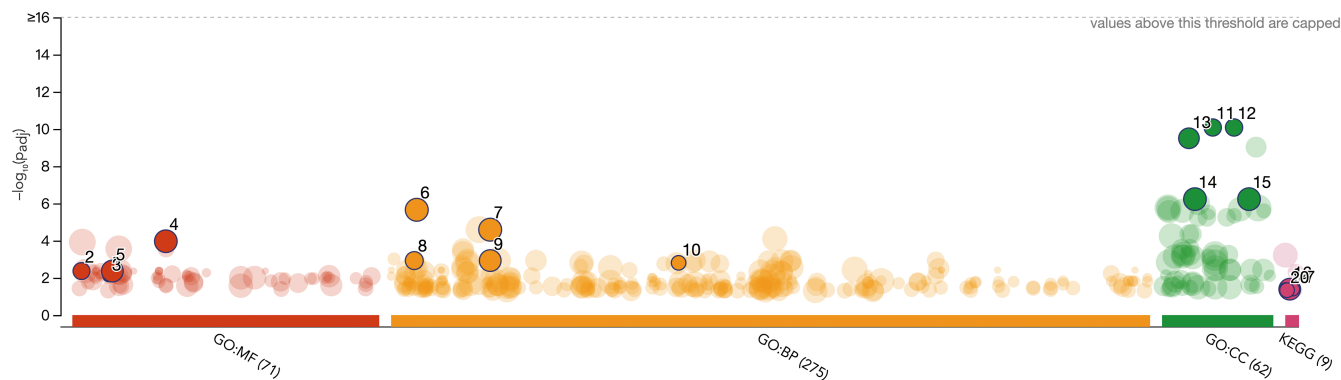
FIGURE 4 Identification of DEmRNAs and DEmiRNAs. (A) Volcano figure. The mRNAs of significance upregulated were shown with the red dots; the significance downregulated mRNAs were shown with the green dot. Fold-change >2.0 and adjusted p -Values <0.05 was significantly different. (B) mRNAs with differential expression between the two groups were analyzed via hierarchical clustering. (C) Venn plot. Prediction and screening for overlapped miRNA. (D) Box plot. Differentially upregulated expressed mRNA between the BPD and non-BPD group.

According to Cellular Component (CC), these DEmRNAs were primarily associated with “specific granules,” “tertiary granules,” “secretory granules,” “cytoplasmic vesicles,” and “intracellular vesicles.” Molecular function (MF) analyses indicated these DEmRNAs were mainly involved in “interleukin-1, type I, activating receptor activity,” “protease binding,” “interleukin-1 receptor activity,” “hydrolase activity,” and “signalling receptor binding.” Besides, KEGG pathway analysis indicated a strong correlation with “metabolic pathways,” “renin-angiotensin system,” “fatty acid biosynthesis,” “starch and sucrose metabolism,” and “amino sugar and nucleotide sugar metabolism.”

4 | DISCUSSION

Over the past several decades, neonatal health care workers and related researchers devoted themselves to numerous treatments for reducing morbidity and improving the prognosis of BPD, including

increased prenatal corticosteroids, surfactant replacement, and less intrusive breathing support. Unfortunately, none of these techniques could significantly contribute to the reduction of the substantial increases in morbidity or mortality of the disease.³² The failure to unravel the molecular mechanisms behind the pathogenesis is the foremost hurdle to the lack of specific therapies. With the mounting discovery of several non-coding RNAs, including miRNAs, lncRNAs, and circRNAs, more spotlights have been focused on exploring their relationship with BPD. Recent data show that circRNAs and the downstream target genes play crucial roles in various biological processes associated with damage repair after immaturity lung injury.^{7,33,34} Therefore, it is essential to investigate the interactions and regulatory mechanisms of the ceRNA network in the development and progression of BPD. As the primary goal of this study, we employed microarray profiling to identify the circRNA expression profiles in the PBMcs in VLBW infants with moderate to severe BPD at 5–8 days after birth. We constructed a novel circRNA-miRNA-mRNA network (composed of 3 circRNA nodes, 22 miRNA



ID	Source	Term ID	Term Name	Padj (query_1)
1	GO:MF	GO:0004909	interleukin-1, type I, activating receptor activity	4.314×10^{-3}
2	GO:MF	GO:0002020	protease binding	4.314×10^{-3}
3	GO:MF	GO:0004908	interleukin-1 receptor activity	8.119×10^{-3}
4	GO:MF	GO:0016787	hydrolase activity	1.078×10^{-4}
5	GO:MF	GO:0005102	signaling receptor binding	4.314×10^{-3}
6	GO:BP	GO:0002376	immune system process	2.199×10^{-6}
7	GO:BP	GO:0009605	response to external stimulus	2.575×10^{-6}
8	GO:BP	GO:0002274	myeloid leukocyte activation	1.178×10^{-3}
9	GO:BP	GO:0009607	response to biotic stimulus	1.178×10^{-3}
10	GO:BP	GO:0042119	neutrophil activation	1.558×10^{-3}
11	GO:CC	GO:0042581	specific granule	8.295×10^{-11}
12	GO:CC	GO:0070820	tertiary granule	8.295×10^{-11}
13	GO:CC	GO:0030141	secretory granule	3.150×10^{-10}
14	GO:CC	GO:0031410	cytoplasmic vesicle	5.874×10^{-7}
15	GO:CC	GO:0097708	intracellular vesicle	5.874×10^{-7}
16	KEGG	KEGG:01100	Metabolic pathways	4.068×10^{-2}
17	KEGG	KEGG:04614	Renin-angiotensin system	4.068×10^{-2}
18	KEGG	KEGG:00061	Fatty acid biosynthesis	4.068×10^{-2}
19	KEGG	KEGG:00500	Starch and sucrose metabolism	4.611×10^{-2}
20	KEGG	KEGG:00520	Amino sugar and nucleotide sugar metabolism	4.611×10^{-2}

FIGURE 6 GO and KEGG functional enrichment analysis For GO enrichment analysis, three components were employed for demonstrating different levels of biological functions: the molecular function (MF), the biological process (BP), and the cellular component (CC). In addition, the KEGG enrichment analysis was applied to assess the level of gene enrichment in various pathways. Based on the most significant adjusted *p*-Value, the top 5 GO terms and KEGG pathways were selected (*p*.adj < 0.05).

and fungi) were demonstrated with a significantly higher risk of BPD compared with those without sepsis, with the relative risk (RR) ranging from 2.6 (95% CI: 1.5–4.6) to 9.40 (95% CI: 3.83–23.08) among different studies.^{41,42} All these suggest that the inflammation response initially triggered by diverse pathogens could contribute to BPD progression and lead to long-term adverse outcomes.

Alternatively, receptor binding may activate many signaling pathways and critical downstream effector molecules. Numerous studies have confirmed that lung injury is closely associated with the inflammatory factor IL-1 β . Bry et al illustrated this point clearly through the transgenic mouse; the overexpressed IL-1 β in the lung caused a BPD-like phenotype in infant mice, including lung inflammation, alveolar hyperplasia, and airway remodeling during both perinatal and postnatal periods.⁴³ This phenomenon is further exemplified when recombinant IL-1RA blocks IL-1 interaction with its

receptor and attenuates lung injury. This also suggests that IL-1RA should be pursued as a potential target for treating BPD.^{44,45} Liao et al provided additional evidence that recombinant IL-1RA could protect the lungs from injury in a neonatal mouse hyperoxia model of BPD.⁴⁶ Increased IL-1 β led to abnormal alveolar development; on the other hand, recombinant IL-1RA blocked inflammation activation and protected alveolar tissue from structural damage. According to our results, for moderate to severe BPD infants, the significant upregulation of hsa_circ_0057950 and the activation of its downstream target gene—IL1R1 (encoding a cytokine receptor for IL-1 α , IL-1 β , and IL-1 receptor antagonist) could be an important molecule and a potential therapeutic target for the pathogenesis of BPD.

Additionally, we employed KEGG pathway analysis to explore notable signaling pathways in the ceRNA network. Aside from

the fact that the renin-angiotensin system was involved in pulmonary fibrosis and the development of BPD under hyperoxia exposure,⁴⁷ another interesting finding was the enriched metabolic pathway. We inferred these were linked to lung microbes due to more recent data revealing that the abnormal distribution of the microbiota in the lung is inextricably linked to the progression of BPD.^{40,48} Different prenatal and postnatal factors, for instance, chorioamnionitis, antibiotic treatment, mechanical ventilation, the microbial population of the NICU environment, and feeding, could contribute to the abnormal distribution of lung microbiota in preterm infants. Short-chain fatty acids (SCFA) and other microbiome-derived metabolites could stimulate the activation and differentiation of immune cells and regulate the host immune system.^{48,49}

Different signaling pathways that affect the formation and progression of BPD have been confirmed by current research, including the VEGF signaling pathways,⁴⁷ p53 signaling pathways,⁵⁰ TGF- β signaling pathway,⁵¹ MAPK signaling pathways,⁵² and PI3K-Akt signaling pathway.⁵³ In contrast to earlier results, however, no evidence of these signaling pathways was detected in our study. We inferred two main factors might be responsible for this deviation. First, the development of BPD is multidimensional, and the progression of the disease is also dynamic.³⁹ In this study, we collected samples during the infant's first 5–8 days postnatally, which were the early stages of BPD development. During the entire postnatal period, various intrinsic factors and external environments can result in stage-specific differences in metabolites and gene expression profiles depending upon the progression of the disease. These factors include intrauterine inflammatory exposure, anti-inflammatory treatment, hyperoxia exposure, and various late complications. As demonstrated in previous studies, the mRNA expression profile and the enriched pathways changed on the 28th day compared with those on the 5th day postnatally in peripheral blood.²⁷ In our study, the significantly enriched pathways during the early stage were most inflammation-related, consistent with the disease progression pattern of BPD. Another reason for this discrepancy was the difficulty obtaining human pulmonary tissue other than peripheral blood samples. The gene expression profiles of peripheral blood leucocytes cannot entirely replace those of lung tissue. However, some studies demonstrated that proinflammatory cytokines in peripheral blood were associated with the phenotype of BPD.⁵⁴ Numerous recent studies have already used this approach as an alternative to lung tissues to identify novel biomarkers for BPD.²⁷

We acknowledge the limitations of our research. First, in this study, differentially expressed circRNAs were identified in a limited number of infants and should be confirmed in a larger cohort. Additionally, many biological processes' crucial changes are not only manifested by changes in RNA levels but also at DNA and protein levels.⁵⁵ These molecular alterations need to be validated further. Even so, the exact role and molecular mechanism of circRNAs affecting the progression of BPD are yet to be determined.

5 | CONCLUSION

We performed microarray technology to identify different expression profiles of circRNAs in peripheral blood from moderate to severe BPD infants 5–8 days after birth. Hsa_circ_0007054, hsa_circ_0057950, hsa_circ_0050386, and hsa_circ_0120151 were verified by qRT-PCR to be differentially expressed between the two groups. Based on mining data from public databases, we constructed a ceRNA regulatory network, including 3 circRNAs, 22 miRNAs, and 16 mRNAs. Gene ontology enrichment and KEGG pathway analysis revealed that these genes were associated with immune cell activation and cytokine receptor activation, which promote the inflammatory response and lung injury.⁵⁶ Our findings suggest that during the progression of BPD, the substantially altered circRNA expression profiles in PBMCs are linked to immune dysregulation from infection and inflammation in the early stage, further supporting the importance of anti-inflammatory treatment for VLBW infants at high risk of developing BPD. These circRNAs detected from PBMCs were novel ones that differed from previous results in this field. They may be functional as potential biomarkers for diagnosis and targets for treating BPD in the early stages of the disease. With the support of our received municipal funds (reference number: SKJYD2021112), further exploration of these genes and exceptionally functional research will contribute to our deepening understanding of BPD in the future.

ACKNOWLEDGMENTS

Yang Zuming designed the experiment and critically reviewed the statistical methodology and conclusions of the article. Yu Lun collected samples and interpreted the data, performed the major part of the statistical analysis, and wrote the article. Junlong Hu collected data and evaluated some of the methods used for data analysis.

FUNDING INFORMATION

The Suzhou Science and Technology Bureau, 2021, reference number: SKJYD2021112. The Jiangsu Commission of Health, 2019, reference number: F201936. The Suzhou Science and Technology Bureau, 2021, reference number: SKJYD2021112. The Jiangsu Commission of Health, On March 23rd, 2019, reference number: F201936; The Suzhou Science and Technology Bureau, On July 1st, 2021, reference number: SKJYD2021112.

CONFLICT OF INTEREST

For this study, Yang Zuming was fortunate to get financial assistance from the Jiangsu Commission of Health and Yu Lun got fund from the Suzhou Commission of health. Yu Lun, Junlong Hu, and Yang Zuming have no conflicts of interest to declare.

DATA AVAILABILITY STATEMENT

Due to the sensitivity of human data, the data that support the findings of this study are not publicly available, but are available from the corresponding author upon reasonable request.

ORCID

Yu Lun  <https://orcid.org/0000-0002-1846-831X>

REFERENCES

- Owen LS, Manley BJ, Davis PG, Doyle LW. The evolution of modern respiratory care for preterm infants. *Lancet*. 2017;389(10079):1649-1659.
- Bhutta AT, Cleves MA, Casey PH, Cradock MM, Anand KJ. Cognitive and behavioral outcomes of school-aged children who were born preterm: a meta-analysis. *JAMA*. 2002;288(6):728-737.
- Jobe AH, Abman SH. Bronchopulmonary dysplasia: a continuum of lung disease from the fetus to the adult. *Am J Respir Crit Care Med*. 2019;200(6):659-660.
- Kinsella JP, Greenough A, Abman SH. Bronchopulmonary dysplasia. *Lancet*. 2006;367(9520):1421-1431.
- Dénervaud V, Gremlich S, Trummer-Menzi E, Schittny JC, Roth-Kleiner M. Gene expression profile in newborn rat lungs after two days of recovery of mechanical ventilation. *Pediatr Res*. 2015;78(6):641-649.
- Steinhorn R, Davis JM, Göpel W, et al. Chronic pulmonary insufficiency of prematurity: developing optimal endpoints for drug development. *J Pediatr*. 2017;191:15-21.e1.
- Bao TP, Wu R, Cheng HP, Cui XW, Tian ZF. Differential expression of long non-coding RNAs in hyperoxia-induced bronchopulmonary dysplasia. *Cell Biochem Funct*. 2016;34(5):299-309.
- Li S, Teng S, Xu J, et al. Microarray is an efficient tool for circRNA profiling. *Brief Bioinform*. 2019;20(4):1420-1433.
- Lu Y, Li Z, Lin C, Zhang J, Shen Z. Translation role of circRNAs in cancers. *J Clin Lab Anal*. 2021;35(7):e23866.
- Salzman J, Gawad C, Wang PL, Lacayo N, Brown PO. Circular RNAs are the predominant transcript isoform from hundreds of human genes in diverse cell types. *PLoS One*. 2012;7(2):e30733.
- Conn SJ, Pillman KA, Toubia J, et al. The RNA binding protein quaking regulates formation of circRNAs. *Cell*. 2015;160(6):1125-1134.
- Zhao W, Zhang Y, Zhu Y. Circular RNA circ β -catenin aggravates the malignant phenotype of non-small-cell lung cancer via encoding a peptide. *J Clin Lab Anal*. 2021;35(9):e23900.
- Li Z, Ruan Y, Zhang H, Shen Y, Li T, Xiao B. Tumor-suppressive circular RNAs: mechanisms underlying their suppression of tumor occurrence and use as therapeutic targets. *Cancer Sci*. 2019;110(12):3630-3638.
- Saaoud F, Drummer IVC, Shao Y, et al. Circular RNAs are a novel type of non-coding RNAs in ROS regulation, cardiovascular metabolic inflammations and cancers. *Pharmacol Ther*. 2021;220:107715.
- Zhou WY, Cai ZR, Liu J, Wang DS, Ju HQ, Xu RH. Circular RNA: metabolism, functions and interactions with proteins. *Mol Cancer*. 2020;19(1):172.
- McEvoy CT, Jain L, Schmidt B, Abman S, Bancalari E, Aschner JL. Bronchopulmonary dysplasia: NHLBI workshop on the primary prevention of chronic lung diseases. *Ann Am Thorac Soc*. 2014;11(Suppl 3(Suppl 3)):S146-S153.
- Yangi R, Huang H, Zhou Q. Long noncoding RNA MALAT1 sponges miR-129-5p to regulate the development of bronchopulmonary dysplasia by increasing the expression of HMGB1. *J Int Med Res*. 2020;48(5):300060520918476.
- Xue H, Yu F, Zhang X, Liu L, Huang L. circ_0000638 inhibits neodymium oxide-induced bronchial epithelial cell inflammation through the miR-498-5p/NF- κ B axis. *Ecotoxicol Environ Saf*. 2020;195:110455.
- Mao X, Guo Y, Qiu J, et al. Next-generation sequencing to investigate circular RNA profiles in the peripheral blood of preterm neonates with bronchopulmonary dysplasia. *J Clin Lab Anal*. 2020;34(7):e23260.
- Zou Z, Wang Q, Zhou M, et al. Protective effects of P2X7R antagonist in sepsis-induced acute lung injury in mice via regulation of circ_0001679 and circ_0001212 and downstream Pln, Cdh2, and Nprl3 expression. *J Gene Med*. 2020;22(12):e3261.
- Zhang J, Li Y, Qi J, et al. Circ-calm4 serves as an miR-337-3p sponge to regulate Myo10 (myosin 10) and promote pulmonary artery smooth muscle proliferation. *Hypertension*. 2020;75(3):668-679.
- Kho AT, Bhattacharya S, Tantisira KG, et al. Transcriptomic analysis of human lung development. *Am J Respir Crit Care Med*. 2010;181(1):54-63.
- Misra RS, Bhattacharya S, Huyck HL, et al. Flow-based sorting of neonatal lymphocyte populations for transcriptomics analysis. *J Immunol Methods*. 2016;437:13-20.
- Walsh MC, Yao Q, Gettner P, et al. Impact of a physiologic definition on bronchopulmonary dysplasia rates. *Pediatrics*. 2004;114(5):1305-1311.
- Ehrenkranz RA, Walsh MC, Vohr BR, et al. Validation of the national institutes of health consensus definition of bronchopulmonary dysplasia. *Pediatrics*. 2005;116(6):1353-1360.
- Wu KY, Jensen EA, White AM, et al. Characterization of disease phenotype in very preterm infants with severe bronchopulmonary dysplasia. *Am J Respir Crit Care Med*. 2020;201(11):1398-1406.
- Pietrzyk JJ, Kwinta P, Wollen EJ, et al. Gene expression profiling in preterm infants: new aspects of bronchopulmonary dysplasia development. *PLoS One*. 2013;8(10):e78585.
- Dweep H, Sticht C, Pandey P, Gretz N. miRWalk—database: prediction of possible miRNA binding sites by "walking" the genes of three genomes. *J Biomed Inform*. 2011;44(5):839-847.
- Wang X. miRDB: a microRNA target prediction and functional annotation database with a wiki interface. *RNA*. 2008;14(6):1012-1017.
- Tokar T, Pastrello C, Rossos AEM, et al. mirDIP 4.1-integrative database of human microRNA target predictions. *Nucleic Acids Res*. 2018;46(D1):D360-D370.
- Raudvere U, Kolberg L, Kuzmin I, et al. G:profiler: a web server for functional enrichment analysis and conversions of gene lists (2019 update). *Nucleic Acids Res*. 2019;47(W1):W191-W198.
- Soll RF, Edwards EM, Badger GJ, et al. Obstetric and neonatal care practices for infants 501 to 1500 g from 2000 to 2009. *Pediatrics*. 2013;132(2):222-228.
- Cheng HR, He SR, Wu BQ, et al. Deep Illumina sequencing reveals differential expression of long non-coding RNAs in hyperoxia induced bronchopulmonary dysplasia in a rat model. *Am J Transl Res*. 2017;9(12):5696-5707.
- Zhong Q, Wang L, Qi Z, et al. Long non-coding RNA TUG1 modulates expression of elastin to relieve bronchopulmonary dysplasia via sponging miR-29a-3p. *Front Pediatr*. 2020;8:573099.
- Wang Y, Wang X, Xu Q, Yin J, Wang H, Zhang L. CircRNA, lncRNA, and mRNA profiles of umbilical cord blood exosomes from preterm newborns showing bronchopulmonary dysplasia. *Eur J Pediatr*. 2022;181(9):3345-3365.
- Birdsey GM, Dryden NH, Shah AV, et al. The transcription factor erg regulates expression of histone deacetylase 6 and multiple pathways involved in endothelial cell migration and angiogenesis. *Blood*. 2012;119(3):894-903.
- Yuan L, Nikolova-Krstevski V, Zhan Y, et al. Antiinflammatory effects of the ETS factor ERG in endothelial cells are mediated through transcriptional repression of the interleukin-8 gene. *Circ Res*. 2009;104(9):1049-1057.
- Huttlin EL, Bruckner RJ, Paulo JA, et al. Architecture of the human interactome defines protein communities and disease networks. *Nature*. 2017;545(7655):505-509.
- Htun ZT, Schulz EV, Desai RK, et al. Postnatal steroid management in preterm infants with evolving bronchopulmonary dysplasia. *J Perinatol*. 2021;41(8):1783-1796.

40. Tirone C, Pezza L, Paladini A, et al. Gut and lung microbiota in preterm infants: immunological modulation and implication in neonatal outcomes. *Front Immunol*. 2019;10:2910.
41. Liljedahl M, Bodin L, Schollin J. Coagulase-negative staphylococcal sepsis as a predictor of bronchopulmonary dysplasia. *Acta Paediatr*. 2004;93(2):211-215.
42. Anderson-Berry A, Brinton B, Lyden E, Faix RG. Risk factors associated with development of persistent coagulase-negative staphylococci bacteremia in the neonate and associated short-term and discharge morbidities. *Neonatology*. 2011;99(1):23-31.
43. Bry K, Hogmalm A, Bäckström E. Mechanisms of inflammatory lung injury in the neonate: lessons from a transgenic mouse model of bronchopulmonary dysplasia. *Semin Perinatol*. 2010;34(3):211-221.
44. Johnson BH, Yi M, Masood A, et al. A critical role for the IL-1 receptor in lung injury induced in neonatal rats by 60% O₂. *Pediatr Res*. 2009;66(3):260-265.
45. Nold MF, Mangan NE, Rudloff I, et al. Interleukin-1 receptor antagonist prevents murine bronchopulmonary dysplasia induced by perinatal inflammation and hyperoxia. *Proc Natl Acad Sci U S A*. 2013;110(35):14384-14389.
46. Liao J, Kapadia VS, Brown LS, et al. The NLRP3 inflammasome is critically involved in the development of bronchopulmonary dysplasia. *Nat Commun*. 2015;6:8977.
47. Wagenaar GT, Laghmani el H, Fidder M, et al. Agonists of MAS oncogene and angiotensin II type 2 receptors attenuate cardiopulmonary disease in rats with neonatal hyperoxia-induced lung injury. *Am J Physiol Lung Cell Mol Physiol*. 2013;305(5):L341-L351.
48. Kalliomäki M, Kirjavainen P, Eerola E, Kero P, Salminen S, Isolauri E. Distinct patterns of neonatal gut microflora in infants in whom atopy was and was not developing. *J Allergy Clin Immunol*. 2001;107(1):129-134.
49. Dang AT, Marsland BJ. Microbes, metabolites, and the gut-lung axis. *Mucosal Immunol*. 2019;12(4):843-850.
50. Bhattacharya S, Zhou Z, Yee M, et al. The genome-wide transcriptional response to neonatal hyperoxia identifies Ahr as a key regulator. *Am J Physiol Lung Cell Mol Physiol*. 2014;307(7):L516-L523.
51. Chen XQ, Wu SH, Luo YY, et al. Lipoxin a(4) attenuates bronchopulmonary dysplasia via upregulation of let-7c and downregulation of TGF- β (1) signaling pathway. *Inflammation*. 2017;40(6):2094-2108.
52. Mo W, Li Y, Chang W, Luo Y, Mai B, Zhou J. The role of LncRNA H19 in MAPK signaling pathway implicated in the progression of bronchopulmonary dysplasia. *Cell Transplant*. 2020;29:963689720918294.
53. Deng J, Huang Y, Wang Q, et al. Human cytomegalovirus influences host circRNA transcriptions during productive infection. *Virology*. 2021;36(2):241-253.
54. D'Angio CT, Ambalavanan N, Carlo WA, et al. Blood cytokine profiles associated with distinct patterns of bronchopulmonary dysplasia among extremely low birth weight infants. *J Pediatr*. 2016;174:45-51.e5.
55. Kim K, Zakharkin SO, Allison DB. Expectations, validity, and reality in gene expression profiling. *J Clin Epidemiol*. 2010;63(9):950-959.
56. Aumiller V, Balsara N, Wilhelm J, Günther A, Königshoff M. WNT/ β -catenin signaling induces IL-1 β expression by alveolar epithelial cells in pulmonary fibrosis. *Am J Respir Cell Mol Biol*. 2013;49(1):96-104.

SUPPORTING INFORMATION

Additional supporting information can be found online in the Supporting Information section at the end of this article.

How to cite this article: Lun Y, Hu J, Zuming Y. Circular RNAs expression profiles and bioinformatics analysis in bronchopulmonary dysplasia. *J Clin Lab Anal*. 2023;37:e24805. doi:[10.1002/jcla.24805](https://doi.org/10.1002/jcla.24805)